



ELSEVIER

Available online at www.sciencedirect.com

SCIENCE @ DIRECT®

C. R. Physique 5 (2004) 687–698



<http://france.elsevier.com/direct/COMREN/>

Ice: from dislocations to icy satellites/La glace : des dislocations aux satellites de glace

Dislocations and plasticity in ice

François Louchet*

LTPCM/ENSEEG, INP de Grenoble, BP 75, 38402 St Martin d'Hères cedex, France

Available online 12 October 2004

Presented by Guy Laval

Abstract

Possible dislocation Burgers vectors and core structures in ice are discussed, and compared with those in crystals with closely related structures such as semiconductors. Theoretical expressions for dislocation velocities are given, on the basis of microscopic mechanisms in dislocation cores, implicitly including the possible role of protonic disorder and core reconstruction. Macroscopic plastic properties are then examined, such as, for instance, the stress dependence of the strain rate, discussed in terms of dislocation density evolution, and the scale invariance of dislocation avalanches, as shown by acoustic emission. **To cite this article:** *F. Louchet, C. R. Physique 5 (2004).*

© 2004 Académie des sciences. Published by Elsevier SAS. All rights reserved.

Résumé

Dislocations et plasticité dans la glace. Nous discutons les différents vecteurs de Burgers et structures de cœur des dislocations dans la glace, en référence à ceux de cristaux ayant des structures très proches comme les semiconducteurs. Nous donnons des expressions théoriques pour les vitesses de dislocations, basées sur les mécanismes microscopiques dans le cœur des dislocations, incluant implicitement un rôle possible du désordre protonique et de la reconstruction du cœur. Les propriétés macroscopiques sont ensuite examinées, comme la dépendance en contrainte de la vitesse de déformation, discutée en termes d'évolution des densités de dislocations, et l'invariance d'échelle des avalanches de dislocations, mises en évidence par émission acoustique. **Pour citer cet article :** *F. Louchet, C. R. Physique 5 (2004).*

© 2004 Académie des sciences. Published by Elsevier SAS. All rights reserved.

Keywords: Ice; Plasticity; Creep; Dislocations; Protonic disorder; Lattice friction

Mots-clés : Glace ; Plasticité ; Fluage ; Dislocations ; Désordre protonique ; Friction de réseau

1. Introduction

Significant advances in the field of the micromechanisms responsible for ice plasticity were achieved in the 1970s and 1990s. X-rays were extensively used to observe both dislocations and dislocation motion in single crystals under stress, using Lang's topography technique [1]. This technique was significantly improved by the use of synchrotron radiation that allowed much shorter exposure times (for a review see [2]).

* Present address: Laboratoire de glaciologie et de géophysique de l'environnement, CNRS, BP 96, 38402 St Martin d'Hères cedex, France.
E-mail address: louchet@lgge.obs.ujf-grenoble.fr (F. Louchet).

On the other hand, ice plasticity has been investigated at the macroscopic scale for about one and a half centuries [3–10]. Among the main results obtained, one can mention (i) a high plastic anisotropy [8–10]; (ii) a power law stress dependence of the creep rate, with an exponent close to 2 for single crystals, and to 3 for polycrystals; and (iii) a possible role of proton disorder on dislocation mobility.

The aim of the present article is to review most of these results. It tries to give a few tracks that may help in better understanding the relations between dislocation mechanisms and macroscopic plasticity, at scales ranging from the atomic size up to that of the collective behaviour of dislocation groups, taking the strong analogy of ice structure with that of diamond cubic semiconductors as a guideline.

2. Structure and defects in ice crystals

2.1. Ice

Hydrogen atoms in water molecules are covalently bonded to Oxygen atoms. Ordinary Ih ice, found between 0 and $-200\text{ }^{\circ}\text{C}$ and up to pressures of about 100 MPa, consists in a tetracoordinated hexagonal lattice of such water molecules, linked by hydrogen bonding (wurtzite structure) [11], as shown in Fig. 1(a). At a typical temperature of $-20\text{ }^{\circ}\text{C}$, the lattice parameters are $a = 4.519\text{ \AA}$ and $c = 7.357\text{ \AA}$ [7]. The angle between O–H bonds in the isolated water molecule (104.5°) is almost the same as between O–O bonds in ice crystals (109.5°), which favours proton location on O–O bonds. Each bond between neighbour oxygen ions contains a single proton (Fig. 1(a)). There is no long range order in the orientation of these O–H bonds.

The crystallographic structure of Ih ice is closely related to that of its metastable diamond cubic variant Ic, their relationship being similar to that between CPH and FCC metals, or to that between wurtzite compound semiconductors and diamond cubic ones as diamond, Si or Ge.

2.2. Point defects

We shall only focus here on molecular and on protonic defects, as they are the only ones, with impurities, that are liable to affect plastic properties.

Molecular point defects consist in vacancies and interstitials. It is currently agreed from observations of interstitial quench loops [12] that, in contrast with metals, the dominant molecular point defects are interstitials, instead of vacancies, about which very little is known in ice. Formation and migration energies are 0.40 eV and 0.16 eV respectively, for interstitials, to be compared with 0.69 and 0.64 eV for vacancies in Al that are the dominant type of point defects in this case [13]. Adding together formation and migration energies gives a self-diffusion energy E_{sd} of 0.56 eV in ice and 1.33 eV in Aluminium.

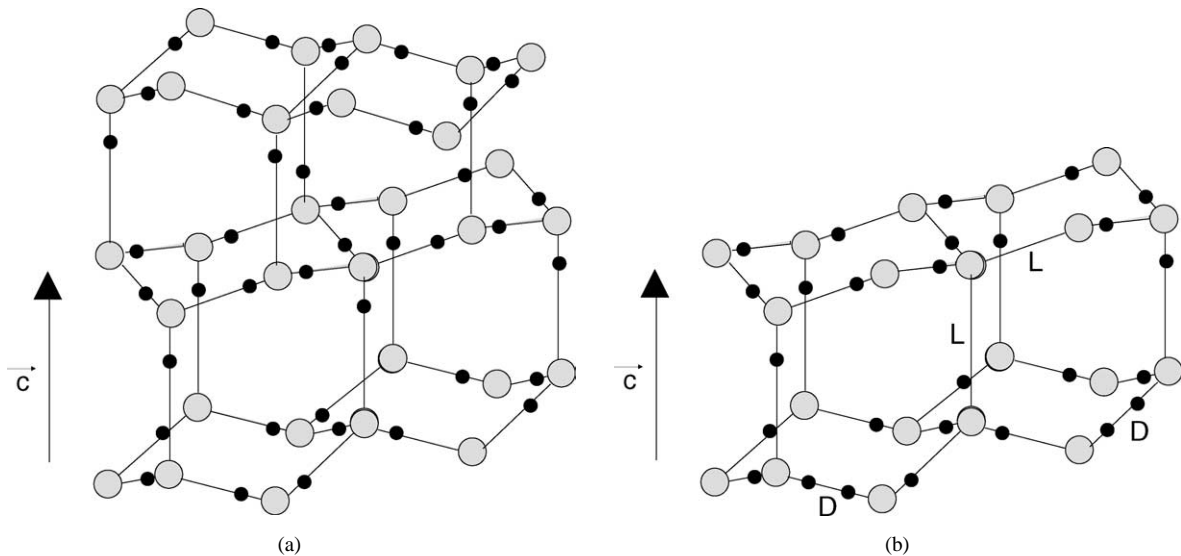


Fig. 1. (a) Hexagonal Ih ice crystal structure: each O–O bond contains one proton in average. There is no long range order in the proton arrangement. (b) Different types of protonic (Bjerrum) defects: proton-free bonds and doubly occupied bonds are respectively labelled L and D.

Taking a melting temperature of about 900 K for Al, the ratio E_{sd}/T_m is 1.86 in ice and 1.47 in Aluminium, which theoretically makes interstitial diffusion in ice slightly, but not drastically more difficult than vacancy diffusion in Al at equivalent temperatures T/T_m .

Since each O–O bond contains one proton in the perfect crystal, rotation of water molecules may lead to violations of these bonding rules, resulting in various ‘protonic point defects’. Bjerrum defects, for instance, correspond to bonds containing either no proton (L-defect), or two protons pointing towards one another (D-defect) (Fig. 1(b)). Such a ‘protonic disorder’ may have consequences for the dislocation motion, and hence for ice plasticity, as detailed later.

2.3. Dislocation structure and motion

The most common dislocation Burgers vectors observed in ice are the three $(a/3)\langle 11\bar{2}0 \rangle$ vectors of the basal plane, as expected from the line energy criterion (the dislocation elastic energy per unit length is proportional to the square of the length of its Burgers vector). A few circular or spiral-shaped prismatic loops with (0001) Burgers vectors were also occasionally observed lying in basal planes [14], and were shown to be formed by the condensation of interstitials [12]. As these dislocations do not seem to participate in plastic deformation, we shall restrict ourselves in the following to dislocations with $(a/3)\langle 11\bar{2}0 \rangle$ Burgers vectors.

Despite reasonable values of the self-diffusion energy, ranging between 0.6 eV and 0.7 eV [15,16], and temperatures rather close to the melting point, no evidence for generalised diffusional plasticity has been reported so far in ice, in contrast with metals. This is likely to be related to the significantly larger E_{sd}/T_m ratio (1.86) in ice as compared to metals, as mentioned in Section 2.2. A further reason, more specific to dislocation climb, may be as follows: the climb velocity of an edge dislocation is given by:

$$V = V_j c_j,$$

where c_j is the jog concentration and V_j the jog climb velocity. The jog formation energy in a metal like Al is fairly small, resulting in sizeable jog concentrations [17]. By contrast, as mentioned hereafter, and based on the argument that basal slip is much easier than non-basal slip, basal dislocations in ice are thought to be widely dissociated in the basal plane. Under this assumption, the formation energy of jogs, that involves a significant contribution of fault constriction, should be high, which may argue against a major and direct contribution of dislocation climb in ice deformation, even at elevated temperatures. However, no direct evidence of such a dissociation has been given so far, and the conclusions given above should be considered with care.

X-Ray or synchrotron radiation topography experiments on ice crystals observed rapidly after unloading [18,19] showed hexagonal-shaped dislocations lying in the basal plane, with $(a/3)\langle 11\bar{2}0 \rangle$ Burgers vectors, and aligned along the three $(a/3)\langle 11\bar{2}0 \rangle$ directions of this plane. One of these three directions corresponds to screw dislocations, and the two others to so-called 60° dislocations. This typical shape is the signature of a lattice friction along these directions. Quite similar shapes are observed in semiconductors (Si, Ge) (Fig. 2) whose diamond cubic crystal structure is strongly related to that of hexagonal ice. This similarity with semiconductors suggests that the origin of the lattice friction in ice is likely to be found in the directional nature of bonding.

As in the case of semiconductors, and owing to the double layer arrangement of Oxygen ions in basal planes (Fig. 3), two sets of dislocations with identical Burgers vectors may exist, depending on whether the extra half plane ends between widely-spaced (shuffle) or narrowly spaced (glide) pairs of basal planes [20]. Dislocations belonging to one set can be transformed into those belonging to the other by absorption or emission of a row of point defects. A glide core may therefore theoretically transform either into a shuffle vacancy or a shuffle interstitial one by climb [21]. In contrast with glide set dislocations that may dissociate into Shockley partial dislocations in the basal plane, dissociation of shuffle dislocations would lead to a high energy stacking fault, and is thus not considered.

Shuffle set dislocation cores contain a single dangling bond per core Oxygen ion, whereas those in the glide set contain three of them. Though this simple argument suggests a higher stability for shuffle cores, the energy reduction associated with a possible dissociation of dislocations of the glide set may stabilise glide dislocations. An essential feature of ice plasticity is the strong predominance of basal slip, which suggests that cross slip onto non-basal planes may be a difficult process. This is a strong argument in favour of widely dissociated dislocations, thus belonging to the glide set rather than to the shuffle set.

The core of a dissociated dislocation loop lying in the basal plane of ice (or in a $\{111\}$ plane in the diamond cubic structure) is schematised in Fig. 4(a). Screw dislocations are dissociated into two 30° Shockley partials, whereas 60° dislocations are dissociated into a 30° and a 90° Shockley partial. Dangling bonds (db) in dislocation cores may possibly reconstruct [22], as shown in Fig. 4(b). Two equivalent reconstruction variants are possible, leading to some ‘antiphase’ sites, called ‘solitons’, and labelled S in Fig. 4(b).

There is reasonable evidence for such a reconstruction in Si and Ge [21]. Covalent bonding indeed provides a strong driving force for core reconstruction in semiconductors, as the pairing of electrons with opposite spins may compensate the energy

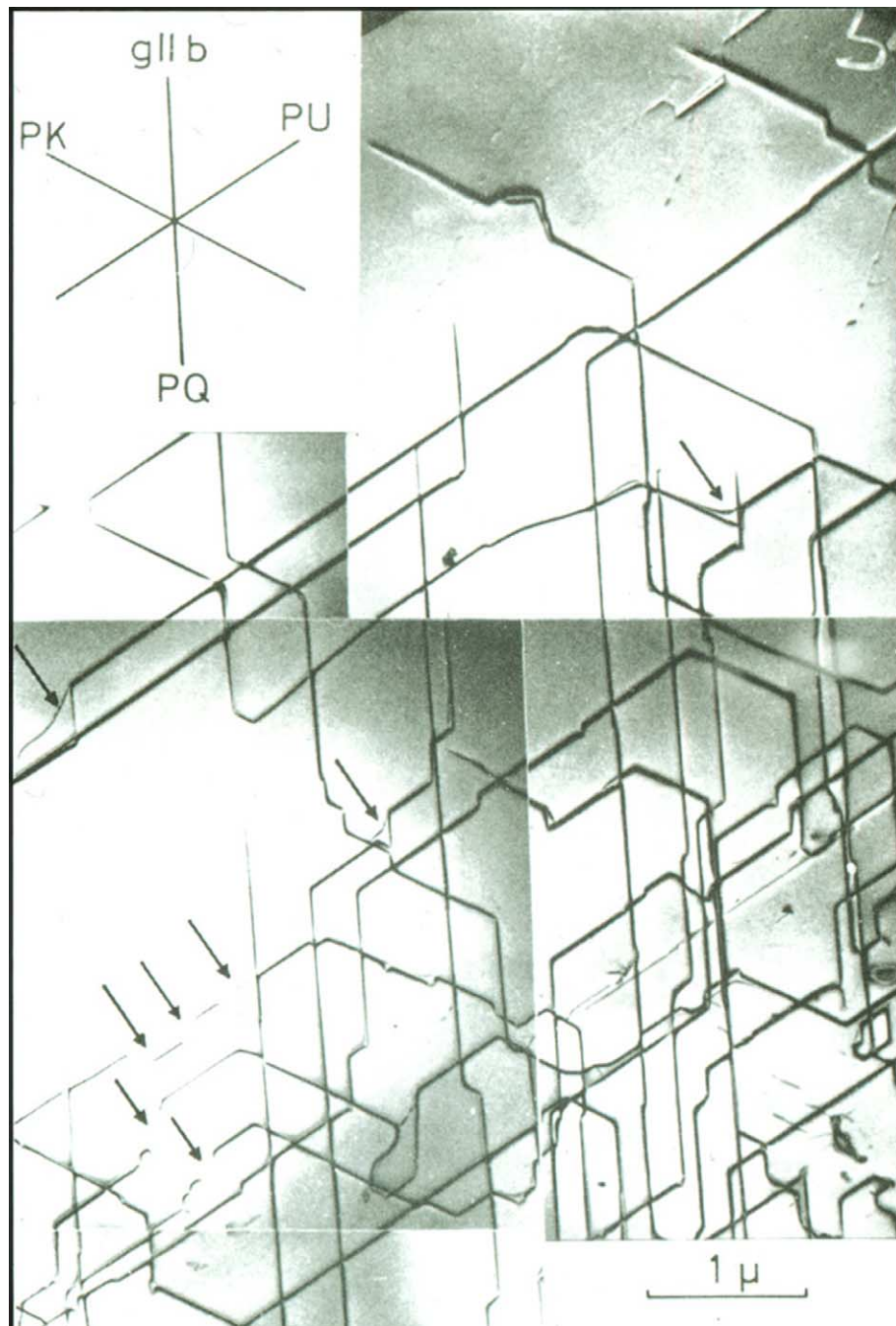


Fig. 2. (a) Typical dislocation arrangement in a $\{111\}$ plane in Si (from [30], with permission from Taylor & Francis). The same hexagonal shapes in the basal planes of ice [18] and in Si suggest that basal dislocations in basal planes of ice have the same core structure as $1/2(110)$ dislocations in $\{111\}$ planes in Silicon.

necessary for bond distortion. The situation is, however, different in ice: since every O–O bond contains a proton, only one half of dangling bonds do so on average, dangling bonds containing protons being distributed at random. Pairing a proton-free db with a proton-decorated db is likely to be favourable, as it reproduces (with some distortion) the normal O–O bond of the bulk crystal, but pairing two proton-free dbs, or even worse two proton-decorated dbs would require energy. Dislocation cores in ice are therefore likely to be either unreconstructed, or partially reconstructed, i.e. containing a high density of solitons. This particular core structure may possibly affect dislocation mobility, as discussed hereafter (Section 3.2).

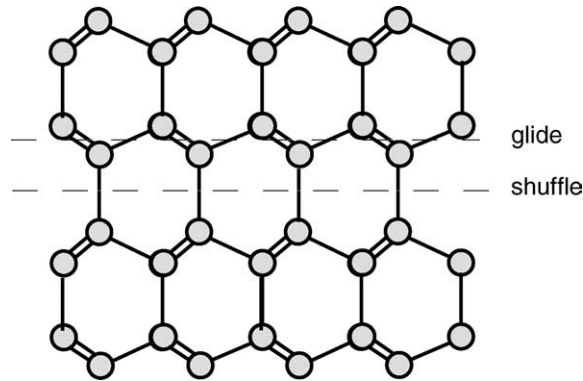


Fig. 3. Ice hexagonal lattice projected along a $(1\bar{2}10)$ direction, with the c -axis vertical, i.e. basal planes horizontal. Bonds lying in the figure plane appear in full length, whereas those sitting out of the figure plane appear in projection as double bonds. Oxygen ions are arranged in basal planes as double layers. An edge dislocation can be schematically constructed by (i) cutting the crystal along the dotted lines; (ii) taking off the atoms contained in the cut zone; and (iii) welding back the crystal. Two sets of dislocations with identical Burgers vectors can be obtained, depending on whether the cut terminates between narrowly (a) or widely (b) spaced basal planes. The corresponding dislocation cores are labelled glide (a) and shuffle (b) sets, respectively.

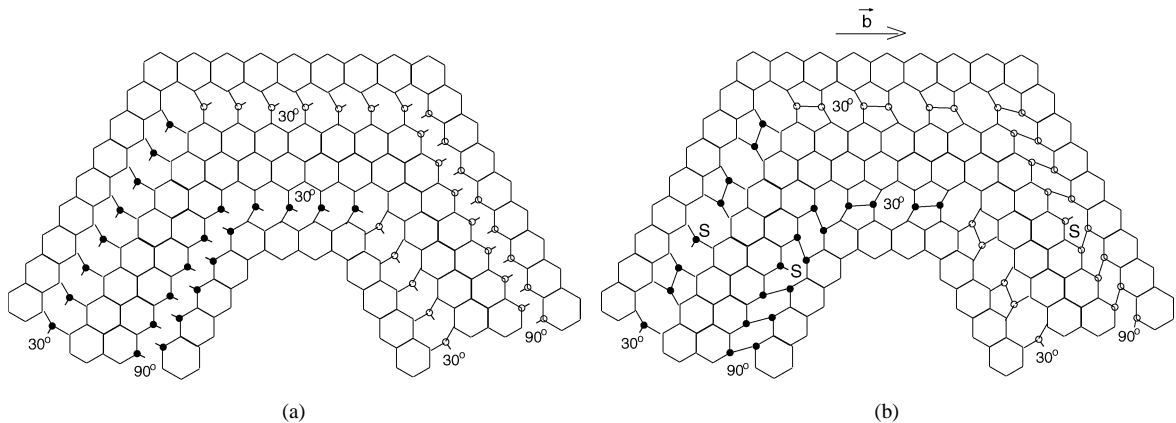


Fig. 4. (a) Schematic cores of a half-dislocation loop in the basal plane with a $\ast(1\bar{2}10)\ast$ Burgers vector, made of one type of screw dislocation (horizontal in the figure) and two types of 60° dislocations. The figure only shows the oxygen ions belonging to the two narrowly spaced basal planes of Fig. 3. Screw dislocations are dissociated into two 30° partials. 60° dislocations are dissociated into a 90° and a 30° partials. (b) Same dislocation loop, with reconstructed cores. Isolated dangling bonds (solitons) are shown on both 90° and 30° partial dislocations.

3. Dislocation mobility

3.1. Basal versus non-basal glide

Optical observations of slip lines by Nakaya [8,9] strongly suggest that basal slip strongly dominates ice plastic activity, resulting in a strong plastic anisotropy. This remains true even for crystal orientations close to those that should inhibit basal slip. Though some prismatic glide is observed for such crystal orientations, no observation of any plastic deformation is reported in crystals loaded along the $[0001]$ direction, that inhibits both basal and prismatic slip. As a consequence, a possible contribution of pyramidal slip to deformation of ice should be considered as negligible.

Dislocation velocity measurements were obtained through sequences of X-ray topographs taken during deformation at different times [18,19,23–26]. Dislocation shapes in ice may change upon unloading, during the time necessary for obtaining topographs. This disadvantage is removed by the use of intense collimated beams from a synchrotron source, that significantly reduces the exposure time. Most of the results reported hereafter were obtained using this technique.

Basal dislocations gliding in basal planes are found to be far more numerous than those propagating in non-basal ones, and are thought to carry most of the plastic deformation, in agreement with Nakaya's slip line observations.

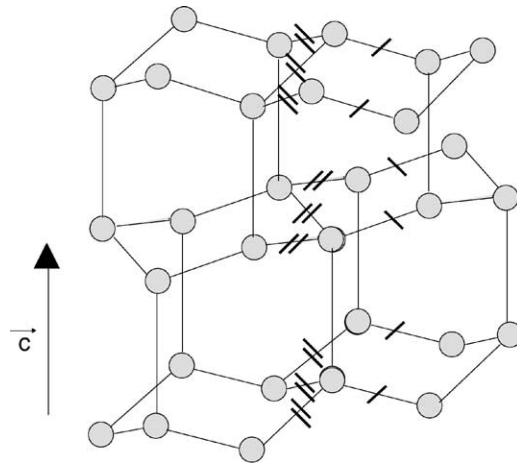


Fig. 5. The propagation in a prismatic plane of an edge dislocation with a basal Burgers vector requires cutting the bonds marked with a double slash for the glide set and with a single slash for the shuffle set. The former requires cutting twice as many bonds than the latter, and this is not balanced by the dissociation energy as it was for dislocations propagating along the basal plane. Edge dislocations propagating in the prismatic plane are therefore likely to belong to the shuffle set.

Screw and 60° dislocations glide with comparable velocities in basal planes. The macroscopic slip direction corresponds to the maximum shear direction in the basal plane [27]. Such an observation may result from the possible combination of the three $(a/3)(\bar{1}\bar{2}10)$ slip directions in the basal plane, with equal critical stresses. The resulting direction should depend in this case on the exponent of the power law relating the strain rate to the stress [28]. The observed result should obviously correspond to a linear stress dependence of the strain rate. However, the observed stress exponent for single crystals is close to 2, as discussed in Section 4.1.

As mentioned above, dislocations with non-basal Burgers vectors are rather uncommon [10]. By contrast, loops with basal $(a/3)(\bar{1}\bar{2}10)$ Burgers vectors and lying in prismatic planes are commonly observed. They are elongated along screw directions, which suggests that screws are much less mobile than edges in these planes. It is indeed agreed that screw dislocations left behind edges do not glide at all in prismatic planes [18], but rather in the intersecting basal planes.

Both the strong plastic anisotropy and the negligible screw mobility in prismatic planes were used to support the idea that basal dislocations should be widely dissociated in basal planes. These views are also supported by determinations of stacking fault energies from the observed shrinkage of prismatic loops [29]. As a consequence, cross-slip from basal to non-basal planes should be rather difficult, resulting in a strong additional barrier for screw motion in non-basal planes: in order to propagate in such planes, dissociated screws should indeed constrict on a critical length, and form a kink pair that would dissociate again in the next valley. This process would require a significant additional energy as compared to the standard energy barrier experienced by screw (and 60°) dislocations propagating in basal planes.

An interesting point is that reported velocities of edges in non-basal planes are between 5 to 10 times larger than those of screws or 60° dislocations in basal planes [25,26,29]. This observation suggests that the nature of lattice friction experienced by non-screw dislocations in basal and in prismatic planes should be somewhat different, which might possibly be understood in terms of the glide or shuffle nature of dislocations. Glide dislocation cores in basal planes correspond to three dangling bonds per atom, instead of a single one for shuffle cores. The excess core energy is nevertheless overbalanced by the dissociation energy for dislocations that lie in the basal plane, which stabilizes the glide core structure. This is also probably the case for screw parts of dislocation loops propagating in prismatic planes, as they also dissociate in basal planes. By contrast, non-screw dislocations lying in prismatic planes cannot dissociate in basal planes since they do not lie in such planes. However, they may also have cores belonging to the equivalents of glide or shuffle sets in prismatic planes. Glide cores in prismatic planes should correspond to two dangling bonds instead of three for basal planes, as one of the four tetrahedral bonds is parallel to the c -axis, i.e. is contained in the prismatic plane (Fig. 5). The corresponding shuffle core only contains one dangling bond per atom, as in basal planes. However, there is no obvious dissociation in prismatic planes, and the energy argument arguing in favour of glide cores instead of shuffle cores in basal planes is no longer valid here: non-screw dislocation cores in prismatic planes should be of a shuffle nature. Propagation of such shuffle dislocations in prismatic planes requires breaking a single O–O bond per atom instead of three for dislocations propagating in basal planes, which corresponds to a significantly lower activation energy. An upper bound of this energy (neglecting the work necessary to drag the half-jog connecting the shuffle edge to the dissociated glide screw) can be roughly estimated as proportional to the number of bonds to be broken, which gives a factor 3 between the former and the latter. This argument should lead to an upper bound of the velocity ratio of about $e^3 \approx 20$, which quite reasonably agrees with the actual velocity ratio (5 to 10).

3.2. Dislocation velocity measurements and modelling

As mentioned in Section 2.2, basal slip in ice involves hexagonal-shaped dislocations [18], which argues for the existence of a significant energy barrier for both kink pair nucleation and kink migration. A very similar situation was first shown in semiconductors, through either topography techniques [30], or Transmission Electron Microscopy (TEM) in situ straining experiments [31,32]. The analogy between dislocation behaviour in ice and in semiconductors is illustrated in Fig. 2.

However, these shapes are observed in ice up to temperatures very close to the melting point (-3°C), which is not observed in semiconductors, in which dislocation shapes become quite isotropic at temperatures above $0.5T_m$.

Measurements of dislocation velocities were performed through sequences of X-ray topographs obtained between successive application of the load [33]. The velocities of screw and 60° dislocations in basal planes, and of edge dislocations in non-basal planes, is proportional to stress, for stresses up to 1 MPa. The temperature dependence of velocities at constant stress obey an Arrhenius law, from which activation energies ΔG can be derived (see Table 1).

These figures given in Table 1 can be compared with 1.33 ± 0.025 eV for screws and 1.40 ± 0.03 eV for 60° dislocations in Ge [34]. With a melting temperature $T_m = 1211.4$ K for Ge, the activation energies normalised by melting temperatures $\Delta G/T_m$ are 3.3×10 eV/K for ice and 1.38×10 eV/K for Ge. This estimate suggests some differences in dislocation core structures of screw and 60° dislocations in ice as compared to semiconductors. The activation energy ΔG involves both the kink formation and migration energies F_k and W_m . The nature of bonding may affect ΔG as a whole, but also its two components F_k and W_m by different amounts. The former effect is responsible for the temperature dependence of dislocation velocities. The latter might be related with the observation of straighter dislocation shapes in ice at high temperatures, as compared with semiconductors. These two effects are tentatively discussed now.

One possible difference between ice and semiconductors may be found in the reconstruction of dangling bonds. If a dislocation core reconstructs spontaneously, the reconstructed structure has to have a lower energy than the non-reconstructed one. This means that potential troughs are deeper, which results in a more difficult kink pair (kp) nucleation and kink propagation. In the case of semiconductors, kink pair nucleation was suggested to take place at solitons [35], as broken bonds are already available there, followed by kink propagation along reconstructed cores. If dislocation cores in ice are badly reconstructed, as stated above, kp nucleation should be as easy as in semiconductors (everything equal), except for the number of competing sites that increases with soliton concentration. In contrast, kink propagation should be easier than in reconstructed semiconductor cores. The number of competing sites affects the prefactor of the Boltzman exponential, whereas the depth of the energy troughs modifies the exponential argument, which usually has a larger effect. These arguments suggest a relatively larger kink propagation versus kp nucleation kinetics in ice as compared to semiconductors, which argues in favour of straighter dislocation shapes at high temperatures in ice, as observed.

Another possible difference should be that proton disorder may present an obstacle to dislocation glide, as first proposed by Glen [36,37]. Shear of one part of the crystal with respect to the other on an intermolecular distance may create Bjerrum defects on about 50% of bonds. 25% of bonds will become expensive doubly occupied D-defects. Reorientation of proton-decorated bonds may prove difficult in the bulk crystal, owing to frustration problems, which might be the reason why such reorientations are usually disregarded. However, the assumption that proton disorder controls dislocation mobilities disagrees with mobility measurements, except if bonds near dislocations are supposed to reorient significantly faster than those in the rest of the crystal (they are supposed to reorient at one half of the dielectric relaxation frequency) [37]. Dislocation propagation indeed affects first neighbour bonds only, and the extra degrees of freedom related to the presence of dangling bonds in dislocation cores may facilitate reorientations, in such a way that only few Bjerrum defects are left in the wake of gliding dislocations. Frustration can also be relieved by proton order defects, as ionic defects, facilitating dislocation glide [38]. Though the role of proton disorder on dislocation mobility is still controversial, it seems that the possible inhibition of bond reconstruction in dislocation cores should make kink propagation easier as compared to semiconductors, and thus have a softening role rather than a hardening one.

Lastly, the assertion that dislocations are straighter in ice than in semiconductors should be tempered by the fact that these high temperature results were obtained using X-ray topography in ice, but Transmission Electron Microscopy (TEM) in semiconductors. These techniques correspond for practical reasons to low strain and dislocation densities in the former case, and high densities in the latter. As dislocation interactions are likely to be responsible for isotropic dislocation shapes in the latter case,

Table 1
Activation energies for velocities of dislocations defects in ice

Dislocation type	Energy (eV)
basal screw	0.95 ± 0.05
basal 60°	0.87 ± 0.04
non-basal edge	0.63 ± 0.04

a similar situation cannot be totally disregarded in ice for large dislocation densities, for which X-ray topography observations are impossible to carry out.

The strong analogy between dislocation behaviour in ice and in semiconductors suggest that they may obey a similar velocity versus stress law. As in other cases of Peierls relief (e.g. [39]), a possible linear dependence of dislocation velocities on their free lengths is expected: the longer the dislocation is, the more numerous the kink pair nucleation sites, and the larger the velocity. Yet, in the case of semiconductors, this dependence should disappear for lengths larger than a critical value: owing to their limited migration rate, kinks of opposite signs may be found simultaneously on long straight dislocations; they propagate in opposite directions, and annihilate at their meeting point, which limits the efficiency of a kink pair nucleation event to the area swept by the kinks before their annihilation. The length dependence of dislocation velocities may thus disappear for dislocation lengths typically larger than the mean free path of kinks $X/2$.

The dislocation velocity V was computed in the case of low stresses by Hirth and Lothe [20]:

$$V = \begin{cases} 2v_D L \frac{\sigma b^3}{kT} \exp\left[-\frac{2F_k + W_m}{kT}\right] & \text{for } L < X, \\ 2v_D b \frac{\sigma b^3}{kT} \exp\left[-\frac{F_k + W_m}{kT}\right] & \text{for } L > X, \end{cases}$$

where W_m and F_k are respectively kink migration and kink formation energies. For the sake of simplicity, both the separation between potential troughs for kink propagation and the kink height are taken equal to the Burgers vector modulus b . The distance swept out along the dislocation by one kink pair before it annihilates with the kinks from other pairs is given by:

$$X = 2\sqrt{\frac{V_k}{J}} = 2b \exp\left(\frac{F_k}{kT}\right),$$

where V_k is the kink velocity, and J the kink pair nucleation rate. This is a typical low-stress approach: considering both forward and backward fluctuations in kp nucleation and expansion, the usual exponential stress dependence valid at large stresses transforms indeed at low stresses into a sinh dependence, that is usually linearised. Such a linear dependence of dislocation velocities on stress is observed experimentally in ice. The maximum value of the sinh argument $\sigma b^3/kT$ obtained at temperatures of the order of 300 K for the maximum stress value reported in velocity measurements (10 MPa) is indeed of about 0.2, i.e. lower than 1, which validates the linearisation.

The length effect mentioned above was reported in semiconductors using in situ straining experiments in a TEM, and allowed separate measurements of kink formation and migration energies [34,40]: in the case of Ge for instance, $F_k = 0.55$ eV for screws and 0.50 eV for 60° dislocations, and $W_m = 0.78$ eV for screws and 0.9 eV for 60° dislocations.

The existence of these two velocity regimes is not mentioned in the literature in the case of ice. Typical values for the critical length X above which dislocation velocities no longer depend on their lengths was shown to be less than 1μ in Si [40] or Ge [34]. As X-ray topographs in ice are taken at much larger scales, it is likely that the observed basal segments have lengths far above the critical value, in spite of the possible relatively larger kink migration rate as compared to kink pair nucleation rate. However, checking the possible existence of a length effect in ice should provide valuable information on the relative values of kink migration and nucleation rates.

4. From dislocation velocities to macroscopic strain rate

4.1. Macroscopic data

4.1.1. Single crystals

The general shape of stress/strain curves, that consist of a yield point followed by a strong softening, is quite similar to those of semiconductors. It is agreed that the upper yield point corresponds with the onset of extensive mobile dislocation multiplication, which results in a significant decrease of their velocities, i.e. of flow stress, at constant strain rate. In the case of semiconductors, the shape of the stress strain curve was modelled either analytically [41] or numerically [42]. However, dislocation multiplication mechanisms in ice may be slightly different [18,19,23,26] as illustrated for instance by the propagation of fast non-basal edge dislocations that create long screw dipoles, which make these models difficult to use directly.

At larger strains, a steady state is reached, corresponding to an almost constant flow stress, i.e. no work hardening. A few reports mention a non-zero work hardening rate at large strains, possibly due to crystal bending [43]. Another possibility should be that the macroscopic strain rate may result from the successive operation of different slip bands, as recently reported [44], a new band being nucleated when the hardening in the last one reaches the nucleation stress of the next one. A non-zero global hardening may appear in this case when the whole specimen is filled with such bands. However, softening at large strains is also reported [45].

Stress–strain curves are reasonably well described using a power law:

$$\dot{\epsilon} \propto \sigma^m \exp(-Q/kT).$$

The activation energy is of about 0.7 eV, and slightly decreases as temperature is increased close to the melting point. The stress exponent m is 2 ± 0.1 in single crystals, from -20°C up to temperatures as high as -0.2°C [43].

4.1.2. Polycrystals

Owing to its large plastic anisotropy, ice can be considered to deform mainly through slip along three coplanar systems, equivalent to two independents ones. It is, however, usually recognised that extensive and homogeneous straining of polycrystals requires the operation of at least five independent slip systems [46,47]. Though, basal and prismatic slip only provide four of them, and pyramidal slip has never been evidenced, as mentioned in Section 3.1. A relaxation of such a homogeneous straining assumption allows compatible deformation of ice polycrystals, at the expense of the development of significant internal stresses [10,48]. These incompatibility stresses (known as kinematic hardening in mechanics) are associated with strong strain gradients, and with the storage of ‘geometrically necessary’ dislocations [49], whose density is expected to be much larger than that of ‘statistical’ dislocations [50,51].

Extensive straining (as observed in polar ice sheets) requires accommodation of these incompatibility stresses, which is thought to occur through grain boundary migration [52]. These views are strongly supported by X-ray diffraction experiments carried out on ice crystals from the Vostok ice core [50,53]. As a consequence, polycrystals deform about a thousand times slower than a single crystal at comparable stresses [10]. The measured stress exponent is 3 at large stresses (0.1 to 10 MPa) [10], but 2 or less at low stresses (lower than 0.1 MPa) [54].

A thorough discussion of plastic deformation in polycrystalline ice is given in [51], to which the reader is referred for more details.

4.2. Mean field approach based on the Orowan equation

The simplest way to derive the constitutive equation from dislocation velocities is the well known mean field approximation that consists in using Orowan’s equation. This type of approach ignores both space and time possible heterogeneities. A precise knowledge of mobile dislocation densities and of their stress and temperature dependences is required for this purpose. Steady state dislocation densities may be obtained from evolution equations, that involve in turn the kinetics of multiplication and annihilation processes.

Deformation of ice crystals involves two types of dislocations with similar $(11\bar{2}0)$ Burgers vectors: edge segments that propagate in non-basal planes, and screw and 60° dislocations that glide in basal planes. Two different rate equations have hence to be written, one for each type of dislocation.

Multiplication of basal dislocations takes place through two main processes [18]:

- (i) edge segments, with basal $(11\bar{2}0)$ Burgers vectors, but gliding in non-basal planes, trail long screw segments behind them. These screw segments can subsequently glide in basal planes, owing to their dislocation in these planes;
- (ii) pole (spiral) sources, sometimes referred to as Frank–Read sources, operate in basal planes, rotating around anchoring points. These anchoring obstacles are the out-of-plane edge segments mentioned above, acting as superjogs on basal dislocations. However, very few sources of this type are observed during synchrotron topography dynamic experiments, dislocation multiplication mainly occurring through mechanism (i), i.e. fast motion of non-basal segments (their velocities are 5 to 10 times larger than those of basal dislocations).

Multiplication of non-basal segments is thought to arise from climb of 60° basal dislocations, rather than from cross slip of screw basal ones [18]. Though, the possibility that they may be generated at surfaces cannot be disregarded.

Elimination of basal dislocations may stem from either pair annihilation of mobile dislocations, locking of mobile dislocations on fixed obstacles, or elimination at surfaces. However, owing to the supposed low cross-slip ability of basal screw dislocations, pair annihilation seems unlikely.

Owing to their reduced lengths and to the presence of long screws trailed behind them, the most obvious elimination process for edge non-basal segments consists of locking on basal dislocations that act as forest obstacles in non-basal glide planes.

Two coupled evolution equations can be written on this basis [55]. Steady state dislocation densities can be found for both non-basal and basal dislocations, that can be introduced in Orowan’s equation. The stress exponent of the strain rate is found to be 2, in agreement with experiments, only if the mutual annihilation of mobile basal dislocations is neglected as compared to locking on obstacles or annihilation at surfaces. This conclusion agrees with the above statement that cross-slip is a difficult process in ice. The only activation energy that remains in the computed strain rate is that related to formation by climb of non-basal segments, and not that corresponding to the propagation of basal nor non-basal dislocations. The experimental findings

that the steady state creep activation energy is between 0.6 and 0.8 eV (Table 8-1 in [7], i.e. in the same range as the self diffusion energy (0.6 to 0.7 eV), agree with the model, the activation energy corresponding to basal dislocation velocities being somewhat larger (0.9 eV).

As dislocation multiplication and annihilation mechanisms are likely to be the same in single crystals and polycrystals, the larger values of the stress exponent in polycrystals for large stresses is not yet understood. They are probably to be related to slip anisotropy and to the resulting incompatibility stresses.

4.3. Long range coupling and deformation dynamics

In contrast with the mean field approach described by Orowan's equation, it is widely agreed that plastic deformation of many materials is heterogeneous in both space and time. Though mean field approaches are usually sufficient to describe the average stress–strain behaviour of materials, it is of interest to explore the profound reasons for such a heterogeneous behaviour. This is also the case for ice, as discussed now.

Since Nakaya's observations of slip patterning in ice single crystals, it is recognised that ice does not deform homogeneously in space. These findings were recently confirmed by measurements of lattice distortions in ice single crystals loaded in torsion [44]. Strain is found to fluctuate along the specimen shaft, thus defining a series of slip bands of different amplitudes. The twist strain corresponding to each band can be described by a regular arrangement of three sets of screw dislocations, generated at the specimen surface, and pushed toward the specimen axis by the applied torsion stress. This dislocation arrangement is geometrically equivalent to a twist boundary, and consists of the geometrically necessary dislocations that accommodate the twist strain [50]. Deformation essentially proceeds through a gradual increase of the number of slip bands. Three-dimensional simulations of dislocation behaviour in ice under torsion conditions [56] may perhaps give further hints for a thorough understanding of slip patterning.

In addition to spatial slip heterogeneities, strain instabilities were also displayed during creep experiments using acoustic emission techniques [57–61]: the amplitude distribution of acoustic waves associated with dislocation avalanches was shown to obey a power law, more clearly shown as a straight line with a negative slope in a double logarithmic plot (Fig. 6). This so-called 'scale-invariance' means that there is no characteristic avalanche size. In other words, the size of the system cannot be determined from the probability distribution function of strain instabilities. It extends over several decades, suggesting that the system is close to a critical state in which the motion of its various components (i.e. dislocations) is correlated over large distances. A small perturbation may result, in this case, in large events.

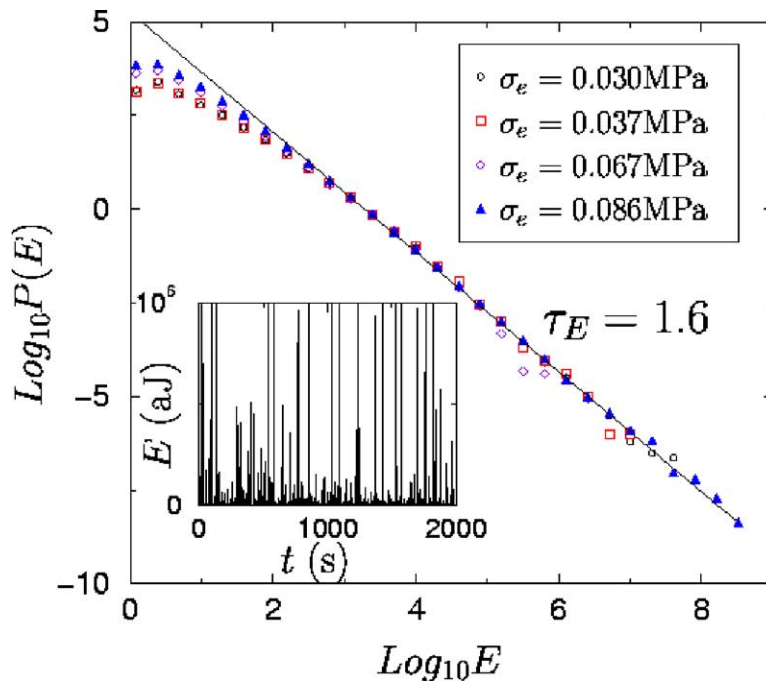


Fig. 6. Distribution of acoustic emission energies of an ice crystal deformed in creep conditions, for different stress levels. It obeys a power law with an exponent 1.6. The time distribution of AE energies (in attoJoules) is also shown.

An interesting feature of this behaviour in ice is that the exponent of the distribution of acoustic emission energies (i.e. the slope of the straight line) is independent of temperature, at least from -20°C up to -3°C [60]. Though the profound reasons for such a behaviour are still to be understood, these findings suggest (as intuitively expected) that the dynamics are controlled by elastic coupling between dislocations rather than by their individual mobilities.

Both space and time avalanche clustering are part of a single phenomenon, that may result from dynamical interactions between avalanches [61]. New avalanches may be more likely to nucleate close to previous ones rather than at random in the crystal. In a same way as dislocations organise into avalanches through their mutual interactions, avalanches organise in turn into spatial and temporal clusters. Yet, the details of dynamical interactions responsible for avalanche clustering are still to be understood.

5. Conclusion

In the present review article, we explored the relations between dislocation mechanisms and macroscopic plasticity, at scales ranging from the atomic size up to that of the collective behaviour of dislocation groups. Ice appears to be quite a particular material, despite the strong analogy of its structure with that of diamond cubic semiconductors. The main conclusions are as follows:

- (i) The high plastic anisotropy of ice agrees with a strong predominance of basal slip and a limited cross slip ability, and suggests a significant dissociation of basal dislocations. This possible dissociation suggests in turn that basal dislocation cores belong to the glide set rather than to the shuffle set.
- (ii) The protonic disorder characteristic of ice crystals is thought to be responsible for a poor bond reconstruction at dislocation cores. The resulting enhanced kink mobility may be responsible for the observed marked hexagonal dislocation shapes up to temperatures very close to the melting point, despite possible artifacts in the comparison of dislocation shapes in ice and semiconductors. Such non-reconstructed cores may also help proton jumps during dislocation motion, avoiding the formation of Bjerrum defects in the dislocation wake. These two remarks suggest that the protonic disorder, instead of being a limiting factor, may favour dislocation mobility, and that dislocation motion may be controlled by lattice friction associated to O–O bonds rather than by protonic disorder.
- (iii) By contrast, basal edges in non-basal planes can hardly dissociate; hence, they probably belong to the shuffle set, in agreement with their much larger mobility.
- (iv) Deformation is ensured by glide of screw and 60° dislocations in basal planes. As for semiconductors, the stress dependence of dislocation velocities is linear at low stresses (< 10 MPa), and results from a kink pair mechanism in a strong Peierls relief.
- (v) Ice obeys a power-law stress dependence of the creep rate. The exponent close to 2 for single crystals may result from a combination of the linear dependence of dislocation velocities with a stationary balance between multiplication and elimination processes of mobile dislocations specific to ice. The larger exponent values reported for polycrystals, whose origin remains unclear, may be related to strain incompatibilities.
- (vi) As for many materials, plasticity of ice is heterogeneous in space and time. It proceeds through dislocation avalanches whose magnitudes are power-law distributed. These avalanches are themselves organised into spatial and temporal clusters.

Acknowledgements

The author is indebted to Drs P. Duval and J. Weiss for fruitful discussions and remarks on the manuscript.

References

- [1] W.W. Webb, C.E. Hayes, *Philos. Mag.* 16 (1967) 909–925.
- [2] A. Higashi (Ed.), *Lattice Defects in Ice Crystals*, Hokkaido University Press, Sapporo, 1988.
- [3] E. Reusch, *Annalen der Physik und Chemie (Poggendorff)* 121 (1864) 573–578.
- [4] J.C. McConnel, *P. Roy. Soc. Lond.* 49 (1891) 323–343.
- [5] J. Weertman, Creep of ice, in: E. Whalley, S.J. Jones, L.W. Gold (Eds.), *Physics and Chemistry of Ice*, Royal Soc. of Canada, Ottawa, 1973, pp. 320–337.
- [6] W.F. Budd, T.H. Jacka, *Cold Reg. Sci. Technol.* 16 (1989) 107–144.
- [7] V.F. Petrenko, R.W. Whitworth, *Physics of Ice*, Oxford University Press, 1999.

- [8] U. Nakaya, IAHS Publ. 47 (1958) 22.
- [9] U. Nakaya, US army snow ice and permafrost research establishment, Research Report 28 (1958) 1–46.
- [10] P. Duval, M.F. Ashby, I. Anderman, J. Phys. Chem. 87 (1983) 4066–4074.
- [11] L. Pauling, J. Am. Chem. Soc. 57 (1935) 2680–2684.
- [12] M. Oguro, T. Hondoh, K. Azuma, Interactions between dislocations and point defects in ice crystals, in: A. Higashi (Ed.), Lattice Defects in Ice Crystals, Sapporo, Hokkaido University Press, 1988, pp. 97–128.
- [13] Y. Quéré, Physique des Matériaux, Ellipses, 1988, p. 148.
- [14] M. Oguro, A. Higashi, J. Cryst. Growth 51 (1) (1981) 71–80.
- [15] R.O. Ramsaier, J. Appl. Phys. 38 (1967) 2553–2556.
- [16] D.E. Brown, S.M. George, J. Phys. Chem. 100 (1996) 15460–15469.
- [17] J. Friedel, Dislocations, Pergamon Press, 1964.
- [18] S. Ahmad, R.W. Whitworth, Philos. Mag. A 57 (1988) 749–766.
- [19] S. Ahmad, C. Shearwood, R.W. Whitworth, in: N. Maeno, T. Hondoh (Eds.), Physics and Chemistry of Ice, Hokkaido University Press, Sapporo, Japan, 1992, pp. 492–496.
- [20] J.P. Hirth, J. Lothe, Theory of Dislocations, Krieger, Malabar, FL, 1992.
- [21] F.J. Louchet, Thibault-Desseaux, Rev. Phys. Appl. 22 (1987) 207–219.
- [22] R. Jones, in: A.G. Cullis, D.C. Joy (Eds.), Proceedings Microscopy of Semiconducting Materials Conference, Oxford, 6–12 April 1981, Inst. Phys. Conf. Series No. 60, sect. 1, 1981, pp. 45–50.
- [23] S. Ahmad, M. Ohtomo, R.W. Whitworth, Nature 319 (1986) 659–660.
- [24] C. Shearwood, R.W. Whitworth, J. Glaciol. 35 (1989) 281–283.
- [25] T. Hondoh, H. Iwamatsu, S. Mae, Philos. Mag. A 62 (1) (1990) 89–102.
- [26] C. Shearwood, R.W. Whitworth, Acta Metall. Mater. 41 (1993) 205–210.
- [27] J.W. Glen, M.F. Perutz, J. Glaciol. 2 (1954) 397–403.
- [28] W.B. Kamb, J. Glaciol. 3 (30) (1961) 1097–1106.
- [29] A. Higashi, A. Fukuda, T. Hondoh, K. Goto, S. Amakai, Dislocations in Solids, Yamada Science Foundation, University of Tokyo Press, 1985.
- [30] K. Wessel, H. Alexander, Philos. Mag. 35 (6) (1977) 1523–1536.
- [31] F. Louchet, J. Phys. C 13 (1980) L847.
- [32] F. Louchet, Philos. Mag. A 43 (5) (1981) 1289.
- [33] C. Shearwood, R.W. Whitworth, Philos. Mag. A 64 (1991) 289–302.
- [34] F. Louchet, D. Cochet-Muchy, Y. Bréchet, J. Pélissier, Philos. Mag. A 57 (2) (1988) 327–335.
- [35] M. Heggie, R. Jones, J. Phys. C 1 (1982) 45.
- [36] J.W. Glen, Physik den Kondensierten Materie 7 (1968) 43–51.
- [37] R.W. Whitworth, J.G. Paren, J.W. Glen, Philos. Mag. 33 (3) (1976) 409–426.
- [38] P.J. Fairbrother, M.I. Heggie, R. Jones, Mat. Res. Soc. Symp. Proc. 193 (1990) 171.
- [39] F. Louchet, L.P. Kubin, D. Vesely, Philos. Mag. A 39 (4) (1979) 433–454.
- [40] F. Louchet, in: A.G. Cullis, D.C. Joy (Eds.), Proceedings Microscopy of Semiconducting Materials Conference, Oxford, 6–12 April 1981, Inst. Phys. Conf. Series No. 60, sect. 1, 1981, pp. 35–38.
- [41] H. Alexander, P. Haasen, Solid State Phys. 22 (1968) 27.
- [42] A. Moulin, M. Condat, L.P. Kubin, Acta Mater. 47 (10) (1999) 2879–2888.
- [43] S.J. Jones, J.G. Brunet, J. Glaciol. 21 (85) (1978) 445–455.
- [44] P.B. Hamelin, P. Bastie, Duval, J. Chevy, M. Montagnat, J. Phys. C, in press.
- [45] S.J. Jones, J.W. Glen, J. Glaciol. 8 (1969) 463–473.
- [46] G.W. Groves, A. Kelly, Philos. Mag. 8 (1963) 877–887.
- [47] J.W. Hutchinson, Met. Trans. A 8 (1977) 1465–1469.
- [48] M.F. Ashby, P. Duval, Cold Reg. Sci. Technol. 11 (1985) 285–300.
- [49] M.F. Ashby, Philos. Mag. 13 (1970) 399–424.
- [50] M. Montagnat, P. Duval, P. Bastie, B. Hamelin, Scripta Mat. 49 (2003) 411–415.
- [51] M. Montagnat, P. Duval, C. R. Physique 5 (2004).
- [52] M. Montagnat, P. Duval, Earth Planet. Sci. Lett. 183 (2000) 179–186.
- [53] M. Montagnat, P. Duval, P. Bastie, B. Hamelin, V.Ya. Lipenkov, Earth Planet. Sci. Lett. 214 (2003) 369–378.
- [54] P. Pimienta, P. Duval, V.Ya. Lipenkov, in: Physical Basis of Ice Sheet Modelling, Vancouver, in: AIHS Publ., vol. 170, 1987, pp. 57–66.
- [55] F. Louchet, Philos. Math. Lett., submitted for publication.
- [56] J. Chaussidon, J. Chevy, M. Montagnat, P. Duval, M. Fivel, Colloque Plasticité, Metz University, France, 2004.
- [57] M.-C. Miguel, A. Vespignani, S. Zapperi, J. Weiss, J.-R. Grasso, Nature 410 (2001) 667–671.
- [58] M.-C. Miguel, A. Vespignani, S. Zapperi, J. Weiss, J.-R. Grasso, Mat. Sci. Engrg. A 309/310 (2001) 324–327.
- [59] J. Weiss, J.-R. Grasso, M.-C. Miguel, A. Vespignani, S. Zapperi, Mat. Sci. Engrg. A 309/310 (2001) 360–364.
- [60] T. Richeton, J. Weiss, F. Louchet, Colloque Plasticité, Metz University, France, 2004.
- [61] J. Weiss, D. Marsan, Science 299 (2003) 89–92.